

12. F. L. Eisele and D. J. Tanner, *J. Geophys. Res.* **96**, 9295 (1991).
13. G. Mount, *ibid.* **97**, 2427 (1992).
14. D. Parrish *et al.*, *ibid.* **95**, 1817 (1990).
15. M. Trainer *et al.*, *ibid.* **92**, 11879 (1987).
16. We thank D. Tanner, E. Marovich, and I. Leifer for help during the intercomparison. T. Hendricks of the Hendricks Mining Company provided the site for the instrumentation located at Caribou, CO.

The GT experiment was funded by Office of Exploratory Research, U.S. Environmental Protection Agency, contract R817121, and National Science Foundation grant ATM 9021522, and the AL experiment was funded by the National Oceanic and Atmospheric Administration Radiatively Important Trace Species Program.

13 January 1992; accepted 13 March 1992

## Synthesis and Electronic Transport of Single Crystal $K_3C_{60}$

X.-D. Xiang, J. G. Hou, G. Briceño, W. A. Vareka, R. Mostovoy, A. Zettl,\* Vincent H. Crespi, Marvin L. Cohen

Sizable single crystals of  $C_{60}$  have been synthesized and doped with potassium. Above the superconducting transition temperature  $T_c$ , the electrical resistivity  $\rho(T)$  displays a classic metal-like temperature dependence. The transition to the superconducting state at  $T_c = 19.8$  K is extremely sharp, with a transition width  $\Delta T < 200$  mK. In contrast to transport behavior of doped polycrystalline and granular thin films, no anomalous fluctuations are observed near  $T_c$  in single crystal specimens.

The discovery of superconductivity in heavy alkali metal-doped  $C_{60}$  (1) has generated great theoretical and experimental interest. Although many experimental results of doped fullerenes have begun to shed some light on the underlying physics of these unique materials, nearly all previous measurements have been performed on weakly linked polycrystalline (2) or granular thin films samples (3). Reliable measurements on single crystals are essential for establishing intrinsic properties and determining the superconductivity mechanism.

We report here the synthesis and electronic transport measurements of high-quality single crystals of  $K_3C_{60}$ . Measurements of the dc electrical resistivity  $\rho(T)$  show an intrinsic metal-like temperature dependence below room temperature, with an extremely sharp transition to the superconducting ground state at  $T_c = 19.8$  K; no evidence is found for strong fluctuation effects near  $T_c$ . These results are in sharp contrast to the behavior of polycrystalline and thin film samples.

To prepare the undoped crystals, pure  $C_{60}$  powder was first extracted from carbon soot via standard liquid chromatography with an alumina column. The powder was baked at  $250^\circ\text{C}$  under dynamic vacuum for 24 hours and then sealed in quartz tubes with a few hundred torr of argon gas. Sealed tubes were placed in a gradient furnace with the powder held at  $650^\circ\text{C}$ ; crystals formed in the tube at about  $450^\circ\text{C}$ . With this vapor

transport method, crystals with flat, shiny faces up to a few millimeters across could be obtained in a few days. X-ray diffraction studies confirmed the fcc (face-centered-cubic) crystal structure and lattice constant reported previously (4) for solid  $C_{60}$ .

Electrical contacts to the samples were made prior to doping by first evaporating silver onto the crystal surfaces and then attaching gold wires with conducting silver paint. Both Van der Pauw (5) and in line four-probe geometries were employed (with similar results). The mounted samples were then sealed together with fresh potassium metal in a Pyrex glass apparatus with tungsten feedthrough leads. Uniform doping was accomplished using a repetitive high-temperature dope-anneal cycle. First, both the sample and dopant were heated uniformly in a furnace while the sample resistance was continuously monitored. The temperature was raised from room temper-

ature to about  $200^\circ\text{C}$  at a rate of  $6^\circ\text{C}$  per minute. At about  $150^\circ\text{C}$ , the resistance of the sample dropped down to within the measurable range of the ohm meter ( $20$  m $\Omega$ ); thereafter the resistivity of the sample dropped continually to a few hundred m $\Omega$ -cm within a few minutes. The tube was maintained at about  $200^\circ\text{C}$  for approximately one-half hour until the resistance of the sample reached a minimum. At this point the potassium end of the tube was cooled to room temperature and the sample alone was annealed at about  $200^\circ$  to  $250^\circ\text{C}$  overnight. Then the potassium end was reheated to  $\approx 200^\circ\text{C}$  and the sample was further doped until a lower resistivity minimum was reached. The sample alone was then again annealed for several hours. This doping and annealing process was repeated until the resistance reached an equilibrium state. For transport measurements the sample cell was injected with a helium exchange gas to ensure good thermal conduction, and a diode temperature sensor was mounted in the cell adjacent to the crystal.

The dc electrical resistivity  $\rho$  was measured versus temperature for a crystal of  $K_3C_{60}$  (Fig. 1). Crystals from different preparation batches yielded similar results. Near room temperature the resistivity is about  $5$  m $\Omega$ -cm, comparable to that obtained for  $K_3C_{60}$  films at room temperature (1, 3). However, because of geometrical uncertainties associated with the contact pads, the absolute value of the resistivity should be considered reliable only to within a factor of 2. Below room temperature,  $\rho(T)$  falls in a metal-like fashion with distinct curvature. At  $T_c$  the resistivity drops abruptly to zero, with a transition width  $< 200$  mK. The inset in Fig. 1 shows  $\rho(T)$  near  $T_c$  in detail. The temperature has been swept slowly ( $\sim 50$  mK per minute) near the transition temperature showing no difference in  $T_c$  between cooling and warming.

The  $\rho(T)$  behavior shown in Fig. 1 for the single crystal is in contrast to  $\rho(T)$  observed by other groups for potassium-

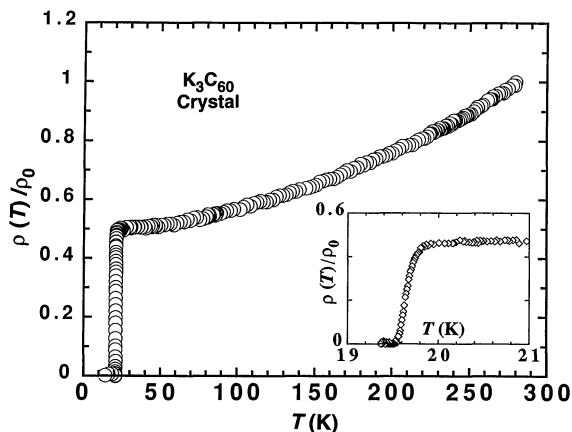


**Fig. 1.** Normalized dc electrical resistivity  $\rho(T)$  for single-crystal  $K_3C_{60}$ . The  $\rho_0$  is the resistivity at  $T = 280$  K. The inset shows the  $\rho(T)$  behavior near the superconducting transition temperature  $T_c = 19.8$  K.

Department of Physics, University of California at Berkeley, and Materials Sciences Division, Lawrence Berkeley Laboratory, Berkeley, CA 94720.

\*To whom correspondence should be addressed.

doped  $C_{60}$  (3, 6). Thin film samples (3) show a semiconductor-like upturn in  $\rho(T)$  above  $T_c$  and a severely broadened transition to the superconducting state. We conclude that this behavior is not intrinsic but due to imperfections such as grain boundaries (3). In fact, our own transmission electron microscopy studies on thin  $C_{60}$  films (7) show that the grain size of freshly deposited films maintained in air at room temperature changes from  $\sim 0.5 \mu\text{m}$  to  $< 200 \text{ \AA}$  over a period of several days. Hence, conclusions drawn from thin film transport data may be suspect.

The quality of our resistivity data and the sharpness of the transition to the superconducting state allow a test of various fluctuation mechanisms. We have attempted to fit  $\rho(T)$  near  $T_c$  to three-, two-, one-, and zero-dimensional fluctuation expressions (8). In all cases, the agreement with experimental data is poor. Hence, we conclude that  $K_3C_{60}$  displays no substantial fluctuation conductivity near the onset to the superconducting state.

The overall temperature dependence of  $\rho(T)$  above  $T_c$  places constraints on normal-state transport models. Preliminary analysis indicates that the temperature dependence of the resistivity can be fit to a  $T^2$  functional form, a result consistent with

electron-electron scattering, although electron-electron scattering has not been observed at such high temperatures in other systems. The observed temperature dependence can also be accounted for with an electron-phonon scattering mechanism (9) if there is a high-frequency contribution from the intraball phonons and a lower frequency contribution from phonons with frequencies in the range of 10 to 200 K.

#### REFERENCES AND NOTES

1. R. C. Haddon *et al.*, *Nature* **350**, 320 (1991).
2. K. Holczer *et al.*, *Science* **252**, 1154 (1991).
3. T. T. M. Palstra, R. C. Haddon, A. F. Hebard, J. Zaanen, *Phys. Rev. Lett.* **68**, 1054 (1992).
4. P. A. Heiney *et al.*, *Phys. Rev. Lett.* **66**, 2911 (1991).
5. L. J. Van der Pauw, *Philips Res. Repts.* **13**, 1 (1958).
6. Y. Maruyama *et al.*, *Chem. Lett.* **10**, 1849 (1991).
7. J. G. Hou *et al.*, in preparation.
8. M. Tinkham, *Introduction to Superconductivity* (Krieger, Huntington, NY, 1975), p. 253.
9. J. M. Ziman, *Electrons and Phonons* (Oxford at the Clarendon Press, Oxford, 1979).
10. This research was supported by National Science Foundation grant DMR88-18404 and by the Office of Energy Research, Office of Basic Energy Sciences, Materials Sciences Division of the U.S. Department of Energy under contract DE-AC03-76SF00098. V.H.C. was supported by a National Defense Science and Engineering Graduate Fellowship.

21 February 1992; accepted 16 April 1992

## Scandium Clusters in Fullerene Cages

Costantino S. Yannoni, Mark Hoinkis, Mattanjah S. de Vries,  
Donald S. Bethune, Jesse R. Salem, Mark S. Crowder,  
Robert D. Johnson

The production and spectroscopic characterization of fullerene-encapsulated metal-atom clusters is reported. In particular, both solution and solid-state electron paramagnetic resonance (EPR) spectra of  $Sc_3C_{82}$  have been obtained.  $ScC_{82}$  also gives an EPR spectrum, but  $Sc_2C_n$  species—the most abundant metallofullerenes in the mass spectrum—are EPR-silent even though  $Sc_2$  is EPR-active in a rare-gas matrix at 4.2 K. The results suggest that the three scandium atoms in  $Sc_3C_{82}$  form an equilateral triangle—as was previously suggested for  $Sc_3$  molecules isolated in a cryogenic rare-gas matrix. The spectrum of  $ScC_{82}$  has features similar to those found earlier for  $LaC_{82}$  and  $YC_{82}$ , suggesting that it can also be described as a +3 metal cation within a -3 fullerene radical anion. An implication of this work is that production of macroscopic quantities of cluster-containing fullerenes may make possible the fabrication of exotic new structures with regular arrays of metal-atom clusters isolated in fullerene molecules, resulting in a new type of host/guest nanostructured material.

The results of carbon cluster-beam experiments (1–5) and the chemical stability recently observed for  $LaC_{82}$  (6, 7),  $La_2C_{80}$  (8),  $YC_{82}$ ,  $Y_2C_{82}$  (9), and  $FeC_{60}$  (10) indicate that entrapping metal atoms in

C. S. Yannoni, M. Hoinkis, M. S. de Vries, D. S. Bethune, J. R. Salem, R. D. Johnson, IBM Research Division, Almaden Research Center, 650 Harry Road, San Jose, CA 95120-6099.  
M. S. Crowder, IBM Adstar, 5600 Cottle Rd., San Jose, CA 95193.

fullerene cages provides a method for isolating and stabilizing reactive species under ambient conditions. We report here the use of this method to obtain spectroscopic data on fullerene-encapsulated metal-atom clusters (11). In particular, both solution and solid-state electron paramagnetic resonance (EPR) spectra of  $Sc_3C_{82}$  have been obtained.  $ScC_{82}$  also gives an EPR spectrum, but  $Sc_2C_n$  species—the

most abundant metallofullerenes in the mass spectrum—are EPR-silent even though  $Sc_2$  is EPR-active in a rare-gas matrix at 4.2 K (12). The results suggest that the three scandium atoms in  $Sc_3C_{82}$  form an equilateral triangle—as was previously suggested for  $Sc_3$  molecules isolated in a cryogenic rare-gas matrix (13). The spectrum of  $ScC_{82}$  has features similar to those found earlier for  $LaC_{82}$  (7), suggesting that it can also be described as a +3 metal cation within a -3 fullerene radical anion. A broader implication of this work is that production of macroscopic quantities of cluster-containing fullerenes may make possible the fabrication of exotic new structures with regular arrays of metal-atom clusters isolated in fullerene molecules, resulting in a new type of host-guest nanostructured material (14).

Metallofullerene samples were prepared by arc-vaporization of 6-mm-diameter graphite rods that were core-drilled and packed with a mixture of scandium metal chips and graphite powder. Arc-burning was carried out in the usual manner in He at 200 torr (3, 15). The soot was collected, extracted with toluene, washed with diethyl ether, and dried. Mass spectra of the extract showed (in addition to  $C_{60}$  and  $C_{70}$ ) several metallofullerenes,  $Sc_mC_n$ , with the diatomic species ( $m = 2$ ,  $80 \leq n \leq 90$ ) in the majority. The principal one- and three-scandium metallofullerene peaks were  $ScC_{82}$  and  $Sc_3C_{82}$ , with the  $C_{84}$  homologs present in lesser quantities. Toluene solutions of this extract were degassed with a freeze-pump-thaw cycle and sealed in quartz tubes for EPR spectroscopy.

The room-temperature EPR spectrum of such a solution is shown in Fig. 1, curve a. Qualitatively, the spectrum appears to be the superposition of two spectra centered around  $g = 2$ , one consisting of eight equally spaced lines of roughly equal intensity and the other a symmetrical pattern of 22 lines, with intensities decreasing monotonically outward from the spectral center. We have been able to simulate the experimental spectrum by superposing simulated EPR spectra with isotropic electron-nuclear hyperfine coupling in species that contain (i) three equivalent scandium nuclei (Fig. 1, curve c) and (ii) a single scandium nuclear spin (Fig. 1, curve d) ( $^{45}Sc$  is 100% abundant with a nuclear spin of 7/2). The spectrum with hyperfine coupling to a single scandium nucleus consists of eight equally spaced lines with equal intensity, while the three-spin simulation generates 22 lines with relative intensities 1:3:6:10:15:21:28:36:42:46:48:48:46:42:36:28:21:15:10:6:3:1. The superposition of Fig. 1, curves c and d, yields the simulation shown in Fig. 1, curve b, in excellent agreement with experiment